Connectivity aware simulated annealing kernel methods for coke microstructure generation

Edward J. Bissaker[1] Bishnu P. Lamichhane[2]
David R. Jenkins[3]

(Received 25 February 2022; revised 12 July 2022)

Abstract

A vital input for steel manufacture is a coal-derived solid fuel called coke. Digital reconstructions and simulations of coke are valuable tools to analyse and test coke properties. We implement biased voxel iteration into a simulated annealing method via a kernel convolution to reduce the number of iterations required to generate a digital coke microstructure. We demonstrate that voxel connectivity assumptions impact the number of iterations and reduce the normalised computation time required to generate a digital microstructure by as much as 70%.

DOI:10.21914/anziamj.v63.17187, Published 2022-07-28, as part of the Proceedings of the 15th Biennial Engineering Mathematics and Applications Conference. ISSN 1445-8810. (Print two pages per sheet of paper.)

Contents

1 Introduction

Metallurgical coke is a porous, high strength carbon material manufactured by heating coal without oxygen. Coke is a key input in a blast furnace, when manufacturing iron from iron ore. Inside a blast furnace, coke serves as a fuel, provides a carbon source to reduce iron oxide and acts as permeable support for the iron ore loaded into the furnace. Coke strength is known to have a significant impact on the performance of coke inside the blast furnace, and industry-standard metrics via tumble drum tests are a standard measure [2]. Coke microstructure features impact its mechanical strength, and hence understanding optimal coke microstructure is a vital tool to manufacture high-performance coke and to increase the efficiency of the iron production process [8]. Quantitative analysis and representation of microstructure are common tools used across various disciplines to understand material structure-property links [11].

The manufacture of coke is an expensive, large scale operation where batches of coke are produced in substantial quantities. It is favourable to explore the material properties of coke without the need for costly manufacture and imaging. An effective, statistically relevant structure generation procedure provides accurate and representative computational models for subsequent analysis of the material's macroscopic properties, and we seek to develop such

a procedure for coke [6].

Torquato et al. [14] provided a framework to generate new structures with spatial statistics corresponding to a measured sample. This technique, commonly referred to as the Yeong–Torquato (Y-T) method, applies a simulated annealing (SA) approach to minimise an energy measure between statistics corresponding to the input and generated structures. In this method, a random binary three-dimensional structure is generated with the appropriate portions of ones and zeros corresponding to the two phases of the material. Two voxels are randomly selected and swapped at each iteration to maintain the appropriate phase volume fractions and alter the structure. This algorithm has been used successfully across various fields and enables the inclusion of a wide range of different spatial statistics. The Y-T procedure has shown reliability and accuracy across many materials [4].

A drawback of the Y-T method is the computational complexity of applying SA to a large 3D cube structure with side length N, containing N^3 voxels. In the Y-T method, the expected number of iterations required grows at least as fast as $\mathcal{O}(\mathsf{N}^3)$, since each voxel may need to be changed multiple times. Evaluating a relevant objective function adds further computation over the entire structure, and the total complexity of the algorithm is approximately $\mathcal{O}(\mathsf{N}^{2\times3})$ [7].

Several different implementations of the Y-T procedure have been devised to improve efficiency across different applications [9]. Biased voxel selection schemes effectively accelerate the Y-T method by reducing the number of voxels that can be selected at a given iteration, thereby reducing the number of iterations and overall computation time to generate a structure [4, 10].

This article presents a biased voxel selection method for digital coke microstructure simulation. We utilise kernel filtering techniques from image processing to implement various voxel connectivity assumptions on the microstructure and reduce the number of iterations required.

Section 2 defines the two-point correlation function and details the Y-T simu-

lated annealing approach for microstructure generation. Section 3 introduces kernel-based image filtering, voxel connectivity, and biased iteration schemes. Section 4 presents some preliminary results from coke microstructure generation across 50^3 and 80^3 voxel structures and 6, 18 and 26 connectivity assumptions. Section 5 discusses the implications of these results and future directions.

2 Microstructure generation via simulated annealing

The two-point correlation function is a spatial statistic that gives the conditional probability that two voxels are in the same phase. It is frequently used to describe the microstructure of various materials and provides information on the large scale features [12].

We consider $\mathcal{A} \in \mathbb{R}^{N\times N\times N}$ to be a three-dimensional digital representation of a coke microstructure from a micro-CT image with $N \in \mathbb{Z}^+$. Usually, a three-dimensional micro-CT image comprises N images of $N \times N$ two-dimensional images. Voxel positions are indexed by j, k, l for each axis. We consider complete segregation of the components into two distinct phases:

1. Ω_1—solid phase voxels;
2. Ω_2—pore phase voxels.

Greyscale image values are converted to binary using an Otsu segmentation applied to each of the N two-dimensional images, where solid and pore phase voxels in $\mathcal{A}$ are given the values 1 and 0, respectively. The phase volume fraction for Ω_i is defined as Φ_i. Hence the solid and pore phases are given by

$$\Phi_1 = \frac{1}{N^3}\sum_{j=1}^{N}\sum_{k=1}^{N}\sum_{l=1}^{N}\mathcal{A}_{j,k,l}\,, \quad \Phi_2 = 1 - \Phi_1\,. \tag{1}$$

The two-point correlation function $s_2^i(\mathbf{r})$ is a microstructure descriptor that

gives the conditional probability that the two points on the ends of a vector $\mathbf{r}$ are in the same phase Φ_i. The two-point correlation function is known to have the properties

$$s_2^i(0) = \Phi_i\,, \quad s_2^i(\infty) = \Phi_i^2\,, \tag{2}$$

for ϕ_i the volume fraction as outlined in (1).

To compute the two-point correlation function on a digital microstructure $\mathcal{A}$, we define a vector

$$\mathbf{r} := \boldsymbol{e}_1 n_1 + \boldsymbol{e}_2 n_2 + \boldsymbol{e}_3 n_3\,,$$

where each $\boldsymbol{e}_k$ is a unit basis vector for $\mathbb{R}^3$ and n_1, n_2, n_3 are positive integers limited by the dimensions of the image N. Hence $\mathbf{r}$ is a vector in $\mathcal{A}$ with end points $\{\mathcal{A}_{j,k,l}, \mathcal{A}_{j+n_1,k+n_2,l+n_3}\}$ at which the phase value is evaluated. We consider periodic boundary conditions on $\mathcal{A}$ for $\mathbf{r}$ and hence for Ω_1:

$$s_2^1(\mathbf{r}) = \frac{1}{N^3} \sum_{j=1}^{N} \sum_{k=1}^{N} \sum_{l=1}^{N} \mathcal{A}_{j,k,l} \mathcal{A}_{j+n_1,k+n_2,l+n_3}\,, \tag{3}$$

which translates $\mathbf{r}$ throughout $\mathcal{A}$. Hence, we consider all possible pairs of voxels of phase Ω_1 separated by the chosen vector $\mathbf{r}$.

Fullwood et al. [3] developed a discrete Fast Fourier Transform (FFT) method to compute $s_2^1(\mathbf{r})$ on $\mathcal{A}$:

$$s_2^1(\mathbf{r}) = \mathcal{F}^{-1}(\bar{\mathcal{F}}(\mathcal{A})\mathcal{F}(\mathcal{A}))\,, \tag{4}$$

where $\mathcal{F}$, $\bar{\mathcal{F}}$ and $\mathcal{F}^{-1}$ are the FFT, complex conjugate of the FFT, and the inverse FFT, respectively. This approach efficiently computes the two-point correlation function for all vectors $\mathbf{r}$ and hence produces the three-dimensional two-point correlation function for $\mathcal{A}$. The FFT method in (4) also implicitly imposes periodic boundary conditions on the structure unless further consideration is made. The two-point correlation function is radially averaged, so that generated structures are similar on average but may differ at the voxel level. This radial averaging is important for generating novel microstructures and

not identical structures [3]. We use the notation $s_2^i(r)$ to denote the radially averaged two-point correlation function.

Microstructure generation via SA seeks to generate a simulated three-dimensional microstructure from a random binary initialisation with correct volume fractions. This binary initialisation becomes the iterated structure that is updated at each iteration. The method is formulated as an 'energy minimisation method', where the energy for our problem is defined as

$$E = \left[s_2^1(r) - \tilde{s}_2^1(r)\right]^2, \tag{5}$$

for $s_2^1(r)$ and $\tilde{s}_2^1(r)$, the radially averaged target and iterated structure two-point correlation functions for Ω_1.

To reduce the energy, two voxels are chosen randomly within the iterated structure, and the voxel values at these positions are reversed (voxel value 1 becomes voxel value 0 and vice versa), giving a new microstructure. The energy E is evaluated on this new microstructure, and the structure is either accepted or rejected based on a probability value determined by the current iteration 'temperature' T_k, which is reduced according to a predetermined cooling schedule [13]. For the comparison of the different connectivity methods, we utilise a consistent initial temperature T_0 and step size δt to reduce the variability in annealing time between the different methods. The cooling schedule for all methods is

$$T_{k+1} = \begin{cases} T_k - \delta t & \text{if } T_k > \delta t, \\ \delta t & \text{if } T_k = \delta t, \end{cases} \tag{6}$$

with $k \in \{0, 1, 2, \ldots\}$ and $\delta t \ll 1$. Hence, the probability of accepting a new microstructure is

$$P_{\text{accept}} := \min\left\{1, \exp\left(\frac{E_{\text{old}} - E_{\text{new}}}{T_k}\right)\right\}, \tag{7}$$

and so the algorithm only accepts a reduction in the energy after a number of iterations determined by the choice of T_0 and δt.

If the microstructure is accepted, then it becomes the new target for voxels phase reversal. If the microstructure is rejected, then we return to the microstructure from the previous iteration, and the process is repeated by selecting two different random voxels.

3 Connectivity and image kernels

In the context of image processing, a kernel or convolution matrix can be used for blurring and edge detection. This is achieved by taking a convolution of the kernel and an image. For $\mathcal{A}$ and ω a kernel, the general expression for a convolution is

$$\tilde{\mathcal{A}}_{j,k,l} = \sum_{m=-a}^{a} \sum_{n=-b}^{b} \sum_{p=-c}^{c} \omega(m,n,p)\mathcal{A}_{j+m,k+n,l+p}\,, \tag{8}$$

for $\tilde{\mathcal{A}}_{j,k,l}$ the filtered image, where $a, b, c \in \mathbb{Z}^+$ and depend on the dimensions of ω. We assume periodic boundary conditions, and hence for edge pixels, the convolution includes voxels from the opposite side of the image. We now discuss how different kernels can be used to incorporate different connectivity assumptions on the microstructure and the iterative scheme.

Connectivity provides information about how each voxel in the generated image relates to the surrounding voxels. We consider typical three-dimensional 6, 18 and 26 connectivity methods between voxels [1], and this requires $a = b = c = 1$ in (8). For biased iteration, we consider a voxel to be *resolved* if all its neighbours are of the same phase. For example, a 6-connected voxel only requires six surrounding voxels (each touching a face of the central voxel) to be in the same phase before being excluded from the iteration, whereas a 26-connected voxel requires twenty-six surrounding voxels to be of the same phase (all face, edge and corner neighbours) before becoming resolved. Hence, as the voxel connectivity increases, we increase the constraint for when a voxel can be excluded from iteration.

Connectivity methods are introduced into the iterative SA scheme using variations of an $\mathbb{R}^3$ kernel matrix $\mathbf{M}_{i+1}$ of ones for the corresponding connectivity i. We refer to each connectivity kernel method as k_i. In the case of k_{26}, $\mathbf{M}_{27}$ contains ones at every entry. Entries corresponding to the corner and edge voxels of $\mathbf{M}_{i+1}$ are changed to zero to implement the different connectivity methods. Hence, applying (8) with $\omega = \mathbf{M}_{i+1}$ we produce the filtered image

$$\tilde{\mathcal{A}}_{j,k,l} = \begin{cases} 0 & \text{voxel and all surrounding voxels are pore phase,} \\ i+1 & \text{voxel and all surrounding voxels are solid phase,} \\ i & \text{voxel has up to } i \text{ solid phase neighbours.} \end{cases} \tag{9}$$

Hence, if a voxel takes the value 0 or $i+1$, the voxel is *resolved* (assumed to be in the correct phase at that iteration) and excluded from the algorithm's random selection. In the case of k_{26}, this method is comparable to initial voxel detection for biased iteration [10].

4 Results

The two-point correlation functions were computed on 50^3 and 80^3 subsets of a 500^3 segmented coke micro-CT image. All simulations across different methods were completed using the same initialisation and SA parameters. Iterations were unrestricted, and the same threshold energy value of 2.5×10^{-4} was used to conclude iterations for all structures. This threshold is somewhat arbitrary but is suitable for comparing iteration efficiency. All biased connected-voxel schemes use the same algorithm, with different kernels being the only variation.

The convergence rates for the algorithm are affected by the various connectivity methods. Figure 1(a) and (b) demonstrate that the original unaltered SA approach requires significantly more iterations to reach convergence, and this extra computational work is evident across both 50^3 and 80^3 structures. There is an immediate reduction in iterations utilising a biased voxel scheme with filtering kernels, with a further reduction in iterations evident with a reduction in the connectivity value. Figure 1(c) and (d) show the target

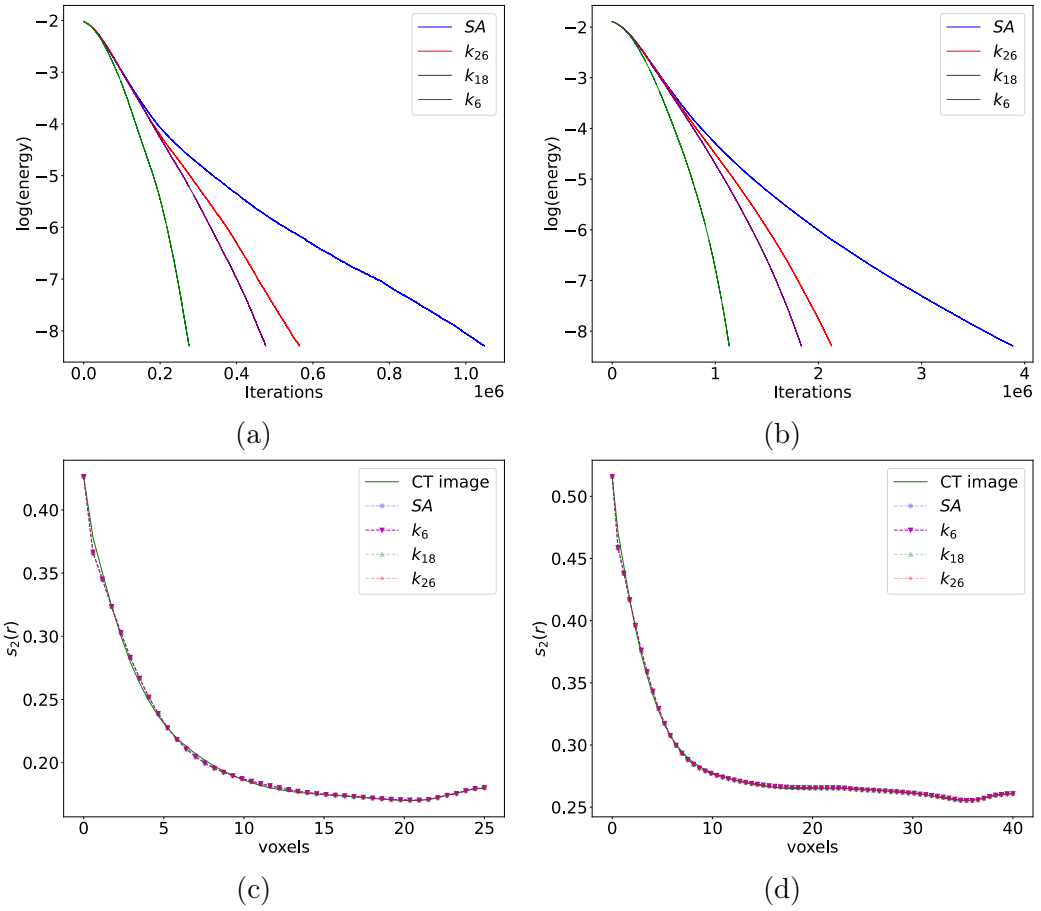

Figure 1: Comparison of the convergence rates and corresponding final radially averaged solid-phase two-point correlation functions for digital microstructure generation with: (a) and (c) 50^3 voxels; (b) and (d) 80^3 voxels. Energy error threshold consistent for all simulations at 2.5×10^{-4}. Voxel size 0.02 mm.

Table 1: Comparison of computational efficiency for each algorithm. Normalised compute time is the product of iterations and the normalised iteration time. The NIT is averaged over 10 runs with 10 000 iterations.

Algorithm	Iterations	NIT	NCT	% SA NCT
	80^3 voxels			
SA	3.88×10^6	1.00	3.89×10^6	100.00
k_{26}	2.13×10^6	1.08	2.29×10^6	59.12
k_{18}	1.83×10^6	1.09	2.00×10^6	51.44
k_6	1.13×10^6	1.08	1.23×10^6	31.52
	50^3 voxels			
SA	1.05×10^6	1.00	1.05×10^6	100.00
k_{26}	5.64×10^5	1.11	6.27×10^5	59.80
k_{18}	4.76×10^5	1.12	5.32×10^5	50.70
k_6	2.76×10^5	1.12	3.10×10^5	29.60

two-point correlation functions are not affected by the connectivity methods and are consistent across all methods.

Table 1 gives higher resolution information about the difference in computation efficiency for the methods. Normalised iteration time for a method k_i is defined as

$$\text{NIT}_{k_i} = \frac{\text{time for single iteration } k_i}{\text{time for single iteration SA}}, \tag{10}$$

and is used to compare the methods since the kernel convolution requires extra computation time (this additional compute time is approximately consistent). Normalised Computation Time NCT_{k_i} is the product of iterations and NIT_{k_i}. Percentage value (%) of SA NCT (see Table 1) quantifies to what extent the overall computation time has been reduced compared to SA. There is a distinct reduction in the percentage value of SA NCT for all kernel methods compared to the SA method. The changes appear consistent across the 50^3 and 80^3 structures. The k_6 method showed a reduction in NCT of 68.48% and 70.4%; k_{27} and k_{18} also reduced by 40.54% and 48.93%, on average.

Figure 2 demonstrates that the generated microstructures show the same qualitative pore and solid-phase distinction as the micro-CT images (Figure 2(a) and (d)). Microstructures produced using the simulated annealing method and the k_6 method show some isolated voxels on the boundary due to the periodicity assumption in kernel computation methods. Hence, a voxel that appears isolated on one boundary is actually 'connected' via the boundary to voxels on the opposing side of the simulation.

5 Discussion and conclusions

The micro-structures generated using connectivity-based kernel voxel bias are quantitively and qualitatively comparable to the original SA method. Due to the modest reduction in iterations required, a connectivity-based voxel selection method can save time generating coke microstructures and make larger sized reconstructions more feasible. Kernels can be updated locally at each iteration around the target voxels, reducing the computational overhead to scale this method to larger structures. It is known that for some materials, the two-point correlation function alone is not sufficient to generate statistically relevant microstructures and capture properties on multiple length scales [5]. Future work will analyse the coke microstructures generated in this work and determine if higher-order statistics are required. Biased voxel methods are compatible with a wide range of spatial statistics [4], and thus the connectivity kernel methods can still be utilised with additional statistics. In summary, the connectivity of voxels can be incorporated into biased iteration schemes using kernel convolution and reduces the required iterations for coke digital microstructure generation.

Acknowledgements The authors acknowledge support for this research through a BHP PhD Research Scholarship.

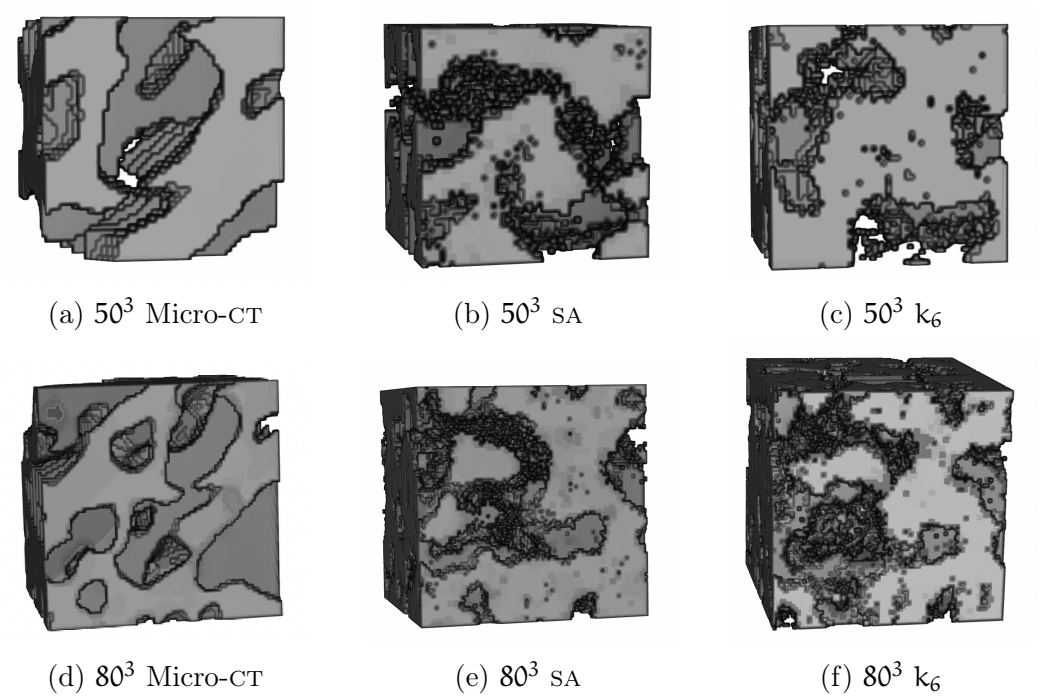

(a) 50^3 Micro-CT (b) 50^3 SA (c) 50^3 k_6

(d) 80^3 Micro-CT (e) 80^3 SA (f) 80^3 k_6

Figure 2: 3D microstructure visualisations. Voxel size 0.02 mm.

References

[1] L. De Floriani, U. Fugacci, and F. Iuricich. "Homological shape analysis through discrete morse theory". In: *Perspectives in Shape Analysis*. Ed. by M. Breuss, A. Bruckstein, P. Maragos, and S. Wuhrer. Springer, 2016, pp. 187–209. DOI: 10.1007/978-3-319-24726-7_9 (cit. on p. C129).

[2] M. A. Diez, R. Alvarez, and C. Barriocanal. "Coal for metallurgical coke production: predictions of coke quality and future requirements for cokemaking". In: *Int. J. Coal Geol.* 50.1–4 (2002), pp. 389–412. DOI: 10.1016/S0166-5162(02)00123-4 (cit. on p. C124).

[3] D. T. Fullwood, S. R. Kalidindi, S. R. Niezgoda, A. Fast, and N. Hampson. "Gradient-based microstructure reconstructions from distributions using fast Fourier transforms". In: *Mat. Sci. Eng. A* 494.1–2 (2008), pp. 68–72. DOI: 10.1016/j.msea.2007.10.087 (cit. on pp. C127, C128).

[4] E.-Y. Guo, N. Chawla, T. Jing, S. Torquato, and Y. Jiao. "Accurate modeling and reconstruction of three-dimensional percolating filamentary microstructures from two-dimensional micrographs via dilation-erosion method". In: *Mat. Character.* 89 (2014), pp. 33–42. DOI: 10.1016/j.matchar.2013.12.011 (cit. on pp. C125, C133).

[5] Y. Jiao, F. H. Stillinger, and S. Torquato. "Modeling heterogeneous materials via two-point correlation functions: Basic principles". In: *Phys. Rev. E* 76.3, 031110 (2007). DOI: 10.1103/PhysRevE.76.031110 (cit. on p. C133).

[6] H. Kumar, C. L. Briant, and W. A. Curtin. "Using microstructure reconstruction to model mechanical behavior in complex microstructures". In: *Mech. Mat.* 38.8–10 (2006), pp. 818–832. DOI: 10.1016/j.mechmat.2005.06.030 (cit. on p. C125).

[7] Z. Ma and S. Torquato. "Generation and structural characterization of Debye random media". In: *Phys. Rev. E* 102.4, 043310 (2020). DOI: 10.1103/PhysRevE.102.043310 (cit. on p. C125).

[8] F. Meng, S. Gupta, D. French, P. Koshy, C. Sorrell, and Y. Shen. "Characterization of microstructure and strength of coke particles and their dependence on coal properties". In: *Powder Tech.* 320 (2017), pp. 249–256. DOI: 10.1016/j.powtec.2017.07.046 (cit. on p. C124).

[9] M. G. Rozman and M. Utz. "Uniqueness of reconstruction of multiphase morphologies from two-point correlation functions". In: *Phys. Rev. Lett.* 89.13, 135501 (2002). DOI: 10.1103/PhysRevLett.89.135501 (cit. on p. C125).

[10] T. Tang, Q. Teng, X. He, and D. Luo. "A pixel selection rule based on the number of different-phase neighbours for the simulated annealing reconstruction of sandstone microstructure". In: *J. Microscopy* 234.3 (2009), pp. 262–268. DOI: 10.1111/j.1365-2818.2009.03173.x (cit. on pp. C125, C130).

[11] S. Torquato. "Microstructure characterization and bulk properties of disordered two-phase media". In: *J. Stat. Phys.* 45.5 (1986), pp. 843–873. DOI: 10.1007/BF01020577 (cit. on p. C124).

[12] S. Torquato and H. W. Haslach Jr. "Random heterogeneous materials: microstructure and macroscopic properties". In: *Appl. Mech. Rev.* 55.4 (2002), B62–B63. DOI: 10.1115/1.1483342 (cit. on p. C126).

[13] S. Torquato and C. L. Y. Yeong. "Reconstructing random media.II: three-dimensional media from two-dimensional cuts". In: *Phys. Rev. E* 58.1 (1998), pp. 224–233. DOI: 10.1103/PhysRevE.58.224 (cit. on p. C128).

[14] C. L. Y. Yeong and S. Torquato. "Reconstructing random media". In: *Phys. Rev. E* 57.1, 495 (1998). DOI: 10.1103/PhysRevE.57.495 (cit. on p. C125).

Author addresses

1. **Edward J. Bissaker**, School of Information and Physical Sciences, University of Newcastle, New South Wales, AUSTRALIA.
mailto:edward.bissaker@newcastle.edu.au
orcid:0000-0002-1608-286X

2. **Bishnu P. Lamichhane**, School of Information and Physical Sciences, University of Newcastle, New South Wales, AUSTRALIA.
mailto:bishnu.lamichhane@newcastle.edu.au
orcid:0000-0002-9184-8941

3. **David R. Jenkins**, School of Engineering, University of Newcastle, New South Wales, AUSTRALIA.

mailto:david.jenkins@newcastle.edu.au
orcid:0000-0001-9660-0585